American Mineralogist, Volume 91, pages 459–462, 2006

LETTER

High-pressure behavior of synthetic antigorite in the MgO-SiO_2-H_2O system from Raman spectroscopy

B. REYNARD[1,*] AND B. WUNDER[2]

[1]Laboratoire de Sciences de la Terre, CNRS UMR 5570, ENS Lyon, 46 Allée d'Italie, F-69364 Lyon Cedex 07, France
[2]GeoForschungsZentrum Potsdam, Department 4 Experimental Geochemistry and Mineral Physics, Telegrafenberg, 14473 Potsdam, Germany

ABSTRACT

The pure synthetic end-member of antigorite was studied by in-situ Raman spectroscopy in a diamond anvil cell. It can be metastably compressed up to 10 GPa at room temperature without occurrence of phase transition or amorphization. The spectrum in the OH region is simpler than in natural antigorite, allowing identification and assignment of the two observed bands at 3672 and 3698 cm^{-1} to the in-phase stretching modes of the outer O3-H3 bonds (brucite-like) and to the stretching mode of the inner O4-H4 bonds (talc-like), respectively. A broad weak shoulder on the low frequency side of the OH bands near 3650 cm^{-1} is better resolved above 7 GPa and assigned to the out-of-phase stretching mode of the outer OH. The two strong OH peaks have small positive pressure dependences (average of 2.3 cm^{-1}/GPa), indicating no enhancement of hydrogen bonding at high pressure. One broad OH band at about 3670 ± 20 cm^{-1} has a large pressure-induced shift (10 ± 2 cm^{-1}). It could be related to structural defects. The specific behavior of OH bands in serpentines can influence the high pressure D/H partitioning with respect to other hydrated minerals.

Keywords: Antigorite, serpentines, hydroxyl in serpentine, stability of antigorite, Raman spectroscopy, high-pressure studies

INTRODUCTION

Serpentine minerals are hydrous phyllosilicates (~13 wt% water) formed during the hydration of ultrabasic and some basic rocks, in particular during hydrothermal alteration of the oceanic lithosphere. They thus have an important role in the global water cycle because they are major water carriers in subduction zones (Iwamori 1998; Scambelluri et al. 1995; Schmidt and Poli 1998; Ulmer and Trommsdorff 1995).

Among serpentine varieties, which are based upon a 1:1 layer structure corresponding to the stacking of layers composed of one tetrahedral and one octahedral sheet, antigorite is characterized by a modulated structure with changes in the layer polarity (Capitani and Mellini 2004; Zussman 1954). Several experimental works demonstrated that antigorite is the stable variety of serpentine under high-pressure conditions (Bose and Ganguly 1995; Ulmer and Trommsdorff 1995; Wunder and Schreyer 1997). This is consistent with its observed abundance in natural serpentinites sampled from high-grade terrains (Auzende et al. 2002; Guillot et al. 2000; Mellini et al. 1987; Scambelluri et al. 1995). Understanding the high-pressure behavior of antigorite is important for constraining its properties at great depths. For instance, vibrational studies can help to understand structural variations, validate ab initio calculations, and model heat capacities and D/H isotopic exchange (Kieffer 1982). In a previous Raman study of serpentines at high pressure (Auzende et al. 2004), distinct behaviors were observed for OH stretching modes, which were attributed to the different OH groups of serpentines. Such a behavior is specific to serpentines and can affect D/H partitioning at high pressure, as observed for brucite (Horita et al. 2002). However, because of the complex structure of OH bands in natural samples and of the presence of Fe and Al substituting for Mg, the origin of these OH bands is still unclear. Thus, the ambient condition Raman spectrum and its high-pressure behavior were investigated in a synthetic pure antigorite (Wunder et al. 1997) and are reported here.

METHODS

The sample is a pure antigorite (sample 287) synthesized at 5 GPa and 500 °C (Wunder et al. 1997). The sample displays broad diffraction peaks indicative of small crystal size and possible mixed structural states, which was confirmed by TEM investigation (Wunder et al. 2001) showing variable value of the modulation *m* between 13 and 20, with a peak value at 18. The sample powder was loaded in a Mao-Bell type diamond anvil cell, equipped with 600 μm culet low-fluorescence diamonds. A 200 μm-diameter hole drilled in a stainless-steel gasket pre-indented at a ~80 μm thickness served as pressure chamber. A 16:4:1 methanol-ethanol-water mixture was used as a pressure-transmitting medium to achieve hydrostatic conditions to 10 GPa, at room temperature. Pressure was determined using the ruby fluorescence (Mao et al. 1986). Raman spectra were recorded in the backscattered geometry, with a Dilor XY double subtractive spectrograph equipped with 1800 gr/mm holographic gratings, and a nitrogen liquid cooled EGG CCD detector. The resolution was 1 cm^{-1}. A microscope with a Mitutoyo Apoplan 50× long-working distance objective was used to focus the incident laser beam (514.5 nm line of an Ar^+ laser) into a 2 μm spot and to collect the Raman signal from the sample. Spectra were acquired over 600 s, with a laser output power of 500 mW.

Shifts of the low frequency bands and of the two narrow OH bands were obtained from spectral deconvolution (Auzende et al. 2004). The third broad band in the OH region was not accurately fitted at pressures below 6 GPa because of the overlap with other bands.

RESULTS AND DISCUSSION

The ambient condition Raman spectrum of synthetic antigorite (Fig. 1), with its low frequency region corresponding to lattice and silicate layer internal vibrational modes, and its high

* E-mail: breynard@ens-lyon.fr

frequency region corresponding to the OH stretching vibrations, is similar to that obtained on a natural sample (Auzende et al. 2004). In the low frequency region, sharp peaks are observed at 132, 229, 378, 459, 688, 1045, and 1098 cm^{-1}. Because of the complexity of the structure, many bands display small splitting, exhibit shoulders, and are broader than in the higher symmetry serpentine variety lizardite (Auzende et al. 2004). This is especially the case for the complex structure assigned to the Si-O-Si bending modes in the 650–700 cm^{-1} region. Shoulders are observed in many peaks from the synthetic sample, but are less resolved than in natural well-ordered antigorite from high pressure terrains, probably because synthetic antigorite is less ordered (Wunder et al. 1997, 2001), but also because of the lower signal-to-noise ratio (Fig. 1). The slight wavenumber differences between synthetic and natural antigorite are attributed to the chemical substitution (Fe and Al mostly) in the natural serpentine, and possibly to orientation effects that can change the relative intensity of slightly split bands. In the high frequency domain (3600–3750 cm^{-1}), the vibrational signal is much simpler in the synthetic than in the natural sample, with two main bands located at 3672 and 3698 cm^{-1}. The position of the first band varies slightly and its relative intensity with respect to the other band varies significantly for different orientations (Fig. 1). This is likely due to the occurrence of many modes with slightly split frequencies in the modulated and low symmetry antigorite structure and to variations in the modulation of antigorite in the experimental charge (Wunder et al. 2001). These structural complexities can also explain the larger bandwidths observed for OH modes in the complex antigorite structure with respect to the higher symmetry lizardite variety. The band frequencies of pure antigorite are in good agreement with those obtained from ab initio calculations (Balan et al. 2002) for the in-phase outer OH stretching mode and the inner OH stretching mode of lizardite, at 3693 and 3726 cm^{-1}, respectively. The contribution for the degenerate out-of-phase outer OH stretching mode, expected at 3655 cm^{-1} from ab initio calculation, is not clearly observed in our experimental spectra. It could correspond to a weak broad shoulder near 3650 cm^{-1} on the low frequency side of the intense OH bands. A shoulder in the highest frequency OH peak is observed at 3693 cm^{-1}. A similar shoulder is observed in the natural antigorite spectrum and is probably due to positional disorder of the inner OH in the distorted silica rings of the tetrahedral layer. A small shoulder at 3701 cm^{-1} is sometimes observed in the synthetic product and attributed to minor chrysotile (Wunder et al. 1997). Additional bands in the spectrum of the natural sample can be explained by various Fe-Al-Mg occupational schemes in the three octahedral sites around the OH group as classically observed in OH-bearing minerals (Burns and Strens 1966). Finally, this assignment of the OH stretching modes in serpentine minerals is consistent with structural refinements of lizardite-1*T* from Val Sissone (Gregorkiewitz et al. 1996; Mellini and Viti 1994) showing that the inner O4-H4 bond (~0.80 Å) is significantly shorter than outer O3-H3 bond (~1.16 Å). Consequently, the contribution of the outer OH bonds should occur at lower frequency than that of the inner OH bonds in the vibrational spectrum of serpentine, in agreement with the assignment proposed from the DFT calculations (Balan et al. 2002).

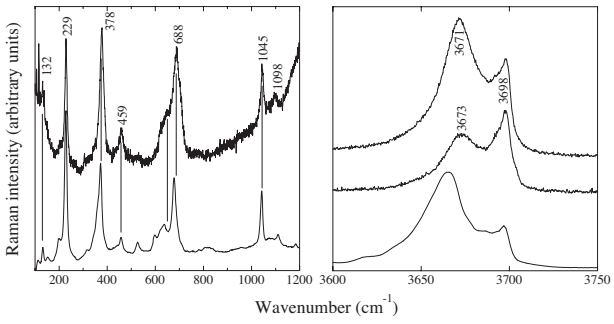

FIGURE 1. Raman spectra of synthetic (left) and natural (right) antigorite at ambient conditions. In the OH region, the two spectra at the top are for two different aggregates of the synthetic crystals with different orientations showing variations of the relative band intensities and slight variation of the lowermost mode frequency. Lower signal-to-noise ratio on the synthetic sample is due to the presence of graphite particles (probably from furnace) that prevent using high laser power because of heating due to light absorption.

The investigated pressure range encompasses the pressure stability field of antigorite (Ulmer and Trommsdorff 1995; Wunder and Schreyer 1997). Upon compression, all Raman bands shift toward higher wavenumbers in the low frequency range as well as in the OH region (Fig. 2, Table 1). Synthetic antigorite still displays well-resolved Raman spectra with no significant line broadening except at 10.9 GPa where the pressure medium solidifies. This indicates that amorphization of antigorite does not occur up to this pressure range for hydrostatic or quasi-hydrostatic conditions. This is in agreement with a high-pressure study of antigorite and lizardite up to 26 GPa at room temperature (Irifune et al. 1996). However, the earlier observation of a gradual amorphization of serpentine between 6 to 22 GPa (Meade and Jeanloz 1991) is probably induced by large non-hydrostatic stresses, as no pressure-transmitting medium was used in that experiment. In the lattice and tetrahedral layer mode region (100–1100 cm^{-1}), five peaks have been followed up to 5 GPa and the observed pressure-induced shifts are equal to those of natural antigorite and other serpentines (Table 1), except for the peak at 688 cm^{-1}, which has a larger pressure dependence than its equivalent in all natural serpentines. This mode is classically

TABLE 1. Pressure dependence of Raman bands of synthetic antigorite and various natural serpentines (Auzende et al. 2004) from linear fits to the data

Lizardite		Chrysotile		Antigorite		Synthetic antigorite	
v_0 (cm^{-1})	dv/dP (cm^{-1}/GPa)	v_0 (cm^{-1})	dv/dP (cm^{-1}/GPa)	v_0 (cm^{-1})	dv/dP (cm^{-1}/GPa)	v_0 (cm^{-1})	dv/dP (cm^{-1}/GPa)
238	4.2(2)	235	4.3(2)	235	4.8(2)	229	4.7(3)
393	3.1(1)	391	3.9(1)	377	4.1(1)	378	3.2(1)
						459	4.6(4)
695	4.1(3)	694	5.0(2)	685	4.9(2)	688	6.5(8)
						1045	4.6(2)
				3619	–0.9(2)		
3654	0.7(1)	3649	1.1(2)	3641	1.2(1)		
3670	8.6(5)	3684	6.6(2)	3643	10.8(2)		
3683	8.8(5)	3689	2.2(1)	3652	10.9(3)	3670(20)	10(2)
3690	8.8(3)	3694	7.1(3)	3661	2.3(1)	3672	2.3(5)
3697	1.1(1)	3698	7.8(1)	3686	2.1(1)		
3706	1.9(1)	3701	2.4(1)	3698	2.6(1)	3698	2.3(1)

Notes: Statistical errors on the last digit given in brackets, except on most zero pressure frequencies, where it is less than the reproducibility of 1 cm^{-1}.

attributed to Si-O-Si bending vibrations in ring, chain, and phyllosilicates. We have no clear explanation for this observation, which suggests a difference in tetrahedral sheet geometry that increases with pressure between synthetic and natural antigorite. It may explain the smaller *P-T* stability range for pure antigorite (Wunder and Schreyer 1997; Wunder et al. 2001) than for natural aluminous antigorite (Bromiley and Pawley 2003).

In the OH region, the two intense peaks at 3672 and 3698 cm^{-1} at ambient pressure are observed at high pressure in the diamond cell (Fig. 2). The 3698 cm^{-1} band shifts by 2.3 cm^{-1}/GPa in the hydrostatic range (0–9.5 GPa), while the 3672 cm^{-1} peak has a slightly smaller linear shift of 1.2(2) cm^{-1}/GPa below 7 GPa and 2.3(5) cm^{-1}/GPa in average from 0 to 9.5 GPa. The positive shift is consistent with the absence of hydrogen bonding for the inner O4-H4 groups. For outer O3-H3 bonds, increase of hydrogen bonding and a negative pressure shift is predicted from Hartree-Fock calculations when reducing the interlayer space upon compression (Benco and Smrcok 1998). It has been proposed that the observed positive shift can be explained if the hydrogen moves toward the center of the sixfold tetrahedral rings while keeping the OH distance constant during compression (Auzende et al. 2004). Finally, a weak band near 3645 cm^{-1} is resolved at the highest pressures (Figs. 2 and 3), but could not be deconvoluted from more intense bands at pressures below 7 GPa, where it corresponds to the weak shoulder near 3650 cm^{-1} observed at ambient pressure. Its shift with pressure is thus small and probably slightly negative. We assign it to the out-of-phase stretching mode of outer OH, for which the position is predicted at 3655 cm^{-1} in lizardite (Balan et al. 2002). DFT calculations are needed to confirm that this particular mode has indeed a slightly negative pressure-induced frequency shift.

At the highest pressures a third intense broad band appears above 3700 cm^{-1} and shifts at a rapid rate of 10 ± 2 cm^{-1}/GPa in average to reach 3775 cm^{-1} at 10.9 GPa (Figs. 2 and 3). The extrapolated ambient-pressure frequency of this band is 3670 ± 20 cm^{-1}; it thus lies under the peak at 3672 cm^{-1} at ambient pressure and could be the explanation for the loss of relative intensity in the 3670–3690 cm^{-1} range as this peak shifts rapidly under pressure, before emerging at higher frequencies than all other OH bands. Such bands with high pressure dependence have also been observed in natural varieties (Auzende et al. 2004). Their occurrence cannot be attributed to the complex chemistry of natural samples because it is observed here in pure antigorite. Such large positive shifts are unusual for OH modes and are not reported in any other high-pressure study of OH-bearing minerals. This band may arise from LO modes of the in-phase vibrations associated with stacking disorder or structural defects as well as morphological effects, as proposed for OH bands in the Raman and infrared spectra of kaolinite (Frost et al. 2001) and other clay minerals (Farmer 2000).

This observation does not change the assignment proposed by Auzende et al. (2004) for outer and inner in-phase OH bands at ambient conditions. However, the simpler structure of the OH region in the pure synthetic sample allows a clear observation that both peaks shift similarly with pressure, as well as confirming the existence of the third OH band with a large pressure shift.

These observations are less clear in natural samples because of additional bands due to Fe and Al substitution for Mg. Occurrence of bands due to the Fe-Mg occupation around the OH groups in natural antigorite can indeed be inferred from the ob-

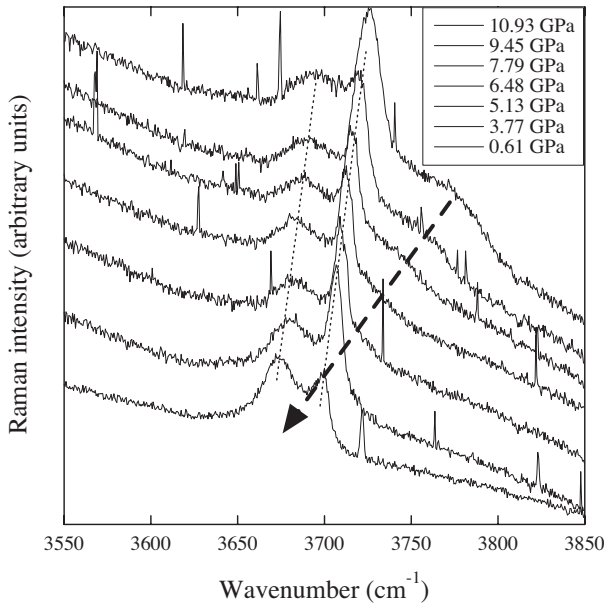

FIGURE 2. High-pressure spectra in the OH stretching mode region, with increasing pressure from bottom to top. Notice the increase of bandwidth at the maximum pressure due to the onset of solidification of the pressure medium. Dotted lines underline the nearly parallel behavior of two OH bands assigned to the in-phase stretching mode of the outer OH and stretching mode of inner OH at 3672 and 3698 cm^{-1}, respectively, while the thick arrow illustrates the strong pressure dependence of a third broad band masked at low pressure under the two former ones. Sharp spikes are noise with random occurrence at high counting times.

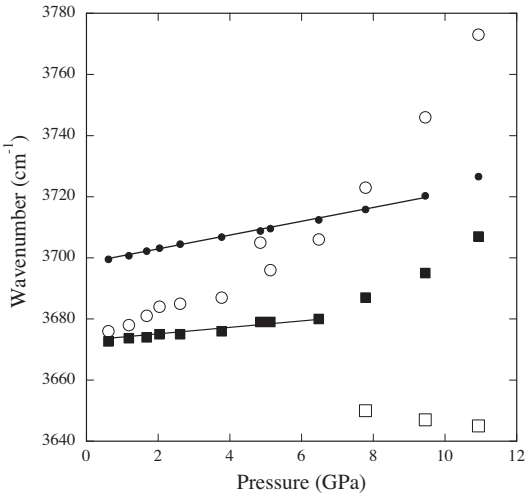

FIGURE 3. Frequency variations of OH bands at high pressure from spectral deconvolution. Non-linear shifts of the 3672 cm^{-1} (filled squares) and broad (open circles) peaks are possibly artifacts of the fitting procedure because of strong overlap below 7 GPa. The position of the 3650 cm^{-1} band assigned to the out-of-phase stretching mode of outer OH (open squares) was fixed to this value below 7 GPa, it is thus reported only above this pressure. Filled circles: stretching mode of the inner OH.

served frequencies and frequency shifts (Auzende et al. 2004). The bands at 3641 and 3619 cm^{-1} have pressure shifts of 1.2 and –0.9 cm^{-1}/GPa, respectively (Table 1) similar to the shifts observed at high pressure in cummingtonite for OH bands corresponding to 2Fe-Mg and 3Fe octahedral neighbors (Yang et al. 1998). They are interpreted as equivalents of the 3Mg octahedral-environment outer OH band at 3672 cm^{-1} in pure Mg-antigorite (Table 1). The weak intensities of these bands are due to the small Fe content of the natural sample and to the statistics of Fe-Mg ordering on octahedral sites (Burns and Strens 1966). With this interpretation and given the composition of the studied natural antigorite, strong OH bands corresponding to 3Mg and 2Mg-Fe octahedral configurations should occur at about 3672 and 3655 cm^{-1}, respectively. The observed complex band with peak frequency at 3661 cm^{-1} is thus attributed to a mixture of these two bands, with additional contribution from the broad bands that shift rapidly with pressure. Similarly, the narrow peak at 3686 cm^{-1} in natural antigorite is attributed to inner OH in a 2Mg-Fe octahedral environment, with a fundamental vibration at 3698 cm^{-1} for 3Mg octahedral environment (Table 1). Contributions from their equivalents for Mg-2Fe and 3Fe octahedral environments would occur around 3674 and 3662 cm^{-1}, assuming a constant negative shift of 12 cm^{-1} each time one Mg is replaced by one Fe for the inner OH mode. Such bands are expected to be weak given the low Fe content, and are masked in the complex and intense 3661 cm^{-1} band composed of the outer modes and broad bands in this region.

The relative simplicity of the OH spectrum observed for the pure Mg-antigorite allows resolving some of the complexities associated with the observation of multiple peaks in the spectra of natural antigorite. It provides tighter constraints for ab initio models, which are restricted to simple compositions. The confirmation of specific behavior of OH modes in serpentines is an important input for attempting vibrational modeling of D/H partitioning between serpentines and water in subduction zone conditions.

ACKNOWLEDGMENTS

This work benefited from the support of the French Institut National des Sciences de l'Univers (program DyETI and Centre de spectroscopie in situ at the ENS Lyon). G Montagnac is thanked for help with Raman spectroscopy. Careful comments from an anonymous reviewer and F.J. Wicks improved the manuscript.

REFERENCES CITED

Auzende, A.L., Devouard, B., Guillot, S., Daniel, I., Baronnet, A., and Lardeaux, J.M. (2002) Serpentinites from Central Cuba: petrology and HRTEM study. European Journal of Mineralogy, 14, 905–914.

Auzende, A.L., Daniel, I., Reynard, B., Lemaire, C., and Guyot, F. (2004) High-pressure behaviour of serpentine minerals: a Raman spectroscopic study. Physics and Chemistry of Minerals, 31, 269–277.

Balan, E., Saitta, A.M., Mauri, F., Lemaire, C., and Guyot, F. (2002) First-principles calculation of the infrared spectrum of lizardite. American Mineralogist, 87, 1286–1290.

Benco, L. and Smrcok, L. (1998) Hartree-Fock study of pressure-induced strengthening of hydrogen bonding in lizardite-1T. European Journal of Mineralogy, 10, 483–490.

Bose, K. and Ganguly, J. (1995) Experimental and theoretical studies of the stabilities of talc, antigorite and phase A at high pressures with applications to subduction processes. Earth and Planetary Science Letters, 136, 109–121.

Bromiley, G.D. and Pawley, A.R. (2003) The stability of antigorite in the systems MgO-SiO_2-H_2O (MSH) and MgO-Al_2O_3-SiO_2-H_2O (MASH): The effects of Al^{3+} substitution on high-pressure stability. American Mineralogist, 88, 99–108.

Burns, R.G. and Strens, R.G.J. (1966) Infrared study of the hydroxyl band in clinoamphiboles. Science, 153, 890–892.

Capitani, G. and Mellini, M. (2004) The modulated crystal structure of antigorite; the $m = 17$ polysome. American Mineralogist, 89, 147–158.

Farmer, V.C. (2000) Transverse and longitudinal crystal modes associated with OH stretching vibrations in single crystals of kaolinite and dickite. Spectrochimica Acta, A56, 927–930.

Frost, R.L., Fredericks, P.M., Kloprogge, J.T., and Hope, G.A. (2001) Raman spectroscopy of kaolinites using different excitation wavelengths. Journal of Raman Spectroscopy, 32, 657–663.

Gregorkiewitz, M., Lebech, B., Mellini, M., and Viti, C. (1996) Hydrogen positions and thermal expansion in lizardite-1*T* from Elba: A low-temperature study using Rietveld refinement of neutron diffraction data. American Mineralogist, 81, 1111–1116.

Guillot, S., Hattori, K., and de Sigoyer, J. (2000) Mantle wedge serpentinization and exhumation of HP rocks: insights from Eastern Ladakh. Geology, 28, 199–202.

Horita, J., Cole, D.R., Polyakov, V.B., and Driesner, T. (2002) Experimental and theoretical study of pressure effects on hydrogen isotope fractionation in the system brucite-water at elevated temperatures. Geochimica et Cosmochimica Acta, 66, 3769–3788.

Irifune, T., Kuroda, K., Funamori, N., Uchida, T., Takehito, Y., Inoue, T., and Miyajima, N. (1996) Amorphization of serpentine at high pressure and high temperature. Science, 272, 1468–1470.

Iwamori, H. (1998) Transportation of H_2O and melting in subduction zones. Earth and Planetary Science Letters, 160, 65–80.

Kieffer, S.W. (1982) Thermodynamics and lattice vibrations of minerals. 5. Application to phase equilibria, isotopic fractionation and high-pressure thermodynamic properties. Reviews in Geophysics and Space Physics, 20, 827–849.

Mao, H., Xu, J., and Bell, P. (1986) Calibration of the ruby pressure gauge to 800 kbar under quasi-hydrostatic conditions. Journal of Geophysical Research, 91, 4763–4767.

Meade, C. and Jeanloz, R. (1991) Deep focus earthquakes and recycling water in the mantle. Science, 252, 68–70.

Mellini, M. and Viti, C. (1994) Crystal structure of lizardite-1*T* from Elba, Italy. American Mineralogist, 79, 1194–1198.

Mellini, M., Trommsdorff, V., and Compagnoni, R. (1987) Antigorite polysomatism: behaviour during progressive metamorphism. Contributions to Mineralogy and Petrology, 97, 147–155.

Scambelluri, M., Müntener, O., Hermann, J., Piccardo, G., and Trommsdorff, V. (1995) Subduction of water in the mantle: history of an Alpine peridotite. Geology, 23, 459–462.

Schmidt, M. and Poli, S. (1998) Experimentally based water budgets for dehydrating slabs and consequences for arc magma generation. Earth and Planetary Science Letters, 163, 361–379.

Ulmer, P. and Trommsdorff, V. (1995) Serpentine stability to mantle depths and subduction-related magmatism. Science, 268, 858–861.

Wunder, B. and Schreyer, W. (1997) Antigorite: high-pressure stability in the system MgO-SiO_2-H_2O. Lithos, 41, 213–227.

Wunder, B., Baronnet, A., and Schreyer, W. (1997) Ab-initio synthesis and TEM confirmation of antigorite in the system MgO-SiO_2-H_2O. American Mineralogist, 82, 760–764.

Wunder, B., Wirth, R., and Gottschalk, M. (2001) Antigorite: Pressure and temperature dependence of polysomatism and water content. European Journal of Mineralogy, 13, 485–495.

Yang, H., Hazen, R.M., Prewitt, C.T., Finger, L.W., Lu, R., and Hemley, R.J. (1998) High-pressure single-crystal X-ray diffraction and infrared spectroscopic studies of the $C2/m$-$P2_1/m$ phase transition in cummingtonite. American Mineralogist, 83, 288–299.

Zussman, J. (1954) Investigation of the crystal structure of antigorite. Mineralogical Magazine, 30, 498–512.

MANUSCRIPT RECEIVED AUGUST 23, 2005
MANUSCRIPT ACCEPTED OCTOBER 28, 2005
MANUSCRIPT HANDLED BY BRYAN CHAKOUMAKOS